JOURNAL OF COMPUTATIONAL PHYSICS 69, 209–229 (1987)

# Sinc Function Computation of the Eigenvalues of Sturm–Liouville Problems

NORMAN EGGERT, MARY JARRATT, AND JOHN LUND*

*Department of Mathematical Sciences, Montana State University, Bozeman, Montana 59717*

Received February 7, 1986; revised July 7, 1986

A collocation scheme using sinc basis functions is developed to approximate the eigenvalues of regular and singular Sturm–Liouville boundary value problems. The error in the approximation of the eigenvalues is shown to converge at the rate $\exp(-\alpha\sqrt{N})$ $(\alpha>0)$, where $2N+1$ basis elements in the collocation scheme are used. A number of test examples are included (both finite and infinite interval boundary value problems) to indicate the accuracy and demonstrate the implementation of the method. © 1987 Academic Press, Inc.

## I. INTRODUCTION

In [7] a sinc-collocation method was developed to approximate the eigenvalues of the Sturm–Liouville boundary value problem

$$\begin{gathered} Lu(x) = -u''(x) + q(x)\,u(x) = \lambda\rho(x)\,u(x), \qquad a<x<b, \\ u(a) = u(b) = 0 \end{gathered} \tag{1.1}$$

in the case that $a=0$ and $b=\infty$. The potential function $q$ is assumed nonnegative and the weight function $\rho$ is taken to be positive. While the method of that paper handled a wide class of singular boundary value problems (the prototype being the radial Schrodinger equation), the discrete system of the method in [7] led to a nonsymmetric matrix eigenvalue problem. The work of this paper is a refinement of the above mentioned work in the sense that the discrete system for the sinc-collocation method of the present paper is symmetric. While the main emphasis of this paper is again the $(0, \infty)$ boundary value problem, there is no distinction between the error estimate for the eigenvalue error bound in the case when $a$ and $b$ are finite and the method is carried out for an arbitrary interval.

Akin to finite difference or finite element approximations (e.g., [10] or [11]) the method of the present paper generates a symmetric positive definite matrix $A$ for the approximation of the eigenvalues of (1.1). In contrast to a banded matrix for the discrete system associated with polynomial based methods, the matrix $A$ is full. However, the rate of convergence of the present method ($(\exp(-\alpha\sqrt{N})$ $(\alpha>0)$

* Work supported by NSF-MONTS Grant ISP-8011449.



0021-9991/87 $3.00

where $2N+1$ basis elements are used) allows one to take smaller discrete systems for equivalent accuracy. Moreover, this exponential rate of convergence is maintained whether or not the eigensolutions of (1.1) are singular. It should be pointed out that, depending on the behavior of $\rho$ and $q$ in (1.1), other methods for the approximation of $\lambda$ are available which also lead to exponential rates of convergence. Indeed, the class of spectral methods [5] yield a technique which for problems (1.1) with analytic solutions converge at a rate faster than any power of $1/N$ where $N$ basis elements are used. Another method for the computation of $\lambda$ in (1.1) can be based on the work in [2]. In this work the mapping of the interval $(a, b)$ to $(-\infty, \infty)$ has been combined with Hermite expansions to yield a method which, for the computation of functions with algebraic singularities, leads to a convergence rate which is $\exp(-\nu\sqrt{N})$ $(\nu > 0)$. Indeed, an example is included in [2] to show that the $\nu$ for the Hermite basis is larger than the $\alpha$ for the sinc basis. All of the methods mentioned in this paragraph when applied to particular problems have their distinct advantages. It is in general quite difficult to assert that "method $x$ is better than method $y$" with no other qualification. The ample numerical testing of a method, even after the convergence of the method has been established, is of immense value to a user who knows what is "better" or even satisfactory for his/her problem. Besides establishing the convergence of this sinc collocation method (Sect. II), the examples of Section III have been selected to indicate both the implementation and performance of the method on problems that either have known solutions or have been discussed elsewhere in the literature.

In Section II the sinc function is defined and the error incured in a sinc expansion approximate to (1.1) is developed. The present work considers only a sinc-collocation scheme although the connection between the latter and a Galerkin scheme may be found in [7] or [12]. The difference between Lu and its sinc expansion evaluated at the sinc nodes gives rise to the generalized eigenvalue problem

$$A\bar{w} = \mu\mathscr{D}^2\bar{w}. \tag{1.2}$$

In (1.2) $A$ is symmetric positive definite and $\mathscr{D}^2$ is a positive definite diagonal matrix. The remainder of Section II bounds the error $|\lambda - \mu|$ where $\mu$ is an eigenvalue of (1.2) and $\lambda$ is an eigenvalue of (1.1). The error in the approximate eigenvector $\bar{w}$ can be carried out in a manner similar to the procedure outlined in [6] and is therefore not included here.

The final Section III is devoted to the numerical method for the computation of $\mu$ in (1.2). The conformal maps which handle the finite interval $(a, b)$ and the half line $(a = 0, b = \infty)$ are summarized in this section. The implementation of the method calls for various parameter selections. A method for the selection of these parameters, based on some elementary asymptotics, is carried out in this section. The section closes with the numerical performance of the method on a number of model problems. On a finite interval the equations of Fourier, Mathieu, and Tschebysheff are considered. On the infinite interval the radial Schrodinger equation with the Harmonic Oscillator, the Laguerre and the Wood–Saxon poten-

tials is computed. The final example, while somewhat nontypical, is included to further distinguish the application of the two conformal maps available for the $(0, \infty)$ boundary value problem.

## II. Sinc Function Approximation

The sinc function is defined by

$$\operatorname{sinc}(t) = \frac{\sin(\pi t)}{\pi t}, \qquad t \in (-\infty, \infty). \tag{2.1}$$

If $w$ is defined on the entire real line then for $h > 0$ the series

$$C(w, h)(t) = \sum_{k=-\infty}^{\infty} w(kh)\, S(k, h)(t), \tag{2.2}$$

where

$$S(k, h)(t) = \operatorname{sinc}\left(\frac{t - kh}{h}\right) \tag{2.3}$$

is called the Whittaker Cardinal expansion of $w$ whenever the series converges. A comprehensive survey of the approximation properties of (2.2) is contained in [13].The properties of (2.2) required for the present work will be briefly summarized in this section.

The class of functions $B(S_d)$, $d > 0$, where the approximation of a function $w$ by its Cardinal expansion is characterized as follows. Let $w \in B(S_d)$ be a function which is analytic in the infinite strip

$$S_d = \{t + is: |s| < d \leqslant \pi/2\} \tag{2.4}$$

and satisfies each of

$$\int_{-d}^{d} |w(t + is)|\, ds \to 0, \qquad t \to \pm\infty \tag{2.5}$$

and

$$N_2(w) = \lim_{s \to d^-} \left( \int_{-\infty}^{\infty} (|w(t + is)|^2 + |w(t - is)|^2)\, dt \right) < \infty. \tag{2.6}$$

An analysis of the error incurred in approximating a function $w \in B(S_d)$ by its Cardinal expansion is found in [13]. For the error in the eigenvalue approximation of this section the truncated expansion of (2.2),

$$C_{M,N}(w, h)(t) = \sum_{k=-M}^{N} w(kh)\, S(k, h)(t), \tag{2.7}$$

and its second derivative

$$\frac{d^2}{dt^2}(C_{M,N}(w,h)(t)) = \sum_{k=-M}^{N} w(kh)\left(\frac{d^2}{dt^2}(S(k,h)(t))\right) \tag{2.8}$$

need to be considered. If $w \in B(S_d)$ then the expansions in (2.7) and (2.8) converge to $w(t)$ and $d^2w/dt^2$, respectively. However, without further assumptions on the rate of growth of $w$ along the real line the expansions require too many terms to be of practical value. In this direction assume that there are positive constants $\alpha$, $\beta$ and $C$ so that

$$|w(t)| \leqslant C \begin{cases} \exp(\alpha t), & t \in (-\infty, 0] \\ \exp(-\beta t), & t \in (0, \infty). \end{cases} \tag{2.9}$$

If $w \in B(S_d)$ and (2.9) is satisfied then, as shown in [13], the two norm error of the second derivative satisfies

$$\left\| \frac{d^2w}{dt^2} - \frac{d^2}{dt^2}(C_{M,N}(w,h)) \right\|_2 \leqslant \left(\frac{\pi}{h}\right)^2 \left\{ \frac{N_2(w)}{\sinh(\pi d/h)} + (C/\sqrt{5h})\left(\frac{e^{-\alpha Mh}}{\alpha} + \frac{e^{-\beta Nh}}{\beta}\right)\right\}. \tag{2.10}$$

If the selections

$$h = (\pi d/\alpha M)^{1/2} \tag{2.11}$$

and

$$N = \left[\!\left[ \frac{\alpha}{\beta} M \right]\!\right] \tag{2.12}$$

are made in the right-hand side of (2.10) then the error is bounded by

$$\left\| \frac{d^2w}{dt^2} - \frac{d^2}{dt^2}(C_{M,N}(w,h) \right\|_2 \leqslant KM^{5/4} \exp(-(\pi\, d\alpha\, M)^{1/2}), \tag{2.13}$$

where $K$ is a positive constant depending on $w$ and $d$. If in (2.9) $\alpha = \beta$ and the selection in (2.11) is retained then the centered approximation

$$C_M(w,h)(t) \equiv C_{M,M}(w,h)(t) = \sum_{k=-M}^{M} w(kh)\, S(k,h)(t) \tag{2.14}$$

yields a second derivative approximation of $d^2w/dt^2$ which is also bounded by the right-hand side of (2.13). While many of the examples of the next section are more efficiently computed using the noncentered approximate ((2.8) with $M \neq N$), the development of the eigenvalue error estimate is notationally more convenient to

develop using (2.14). Before turning to the eigenvalue error estimate, the following definition summarizes the method by which the problem (1.1) is mapped to the entire real line.

DEFINITION 2.1. Let $D_d$ be a simply connected domain in the complex $z = x + iy$ plane with boundary points $a \neq b$ (Fig. 1). Let $\phi$ be a conformal map of $D_d$ onto the infinite strip $S_d$ in (2.4) with $\phi(a) = -\infty$ and $\phi(b) = \infty$. Let the inverse map of $\phi$ be denoted by $\psi$ and define

$$\Gamma = \{\psi(t): -\infty < t < \infty\} \tag{2.15}$$

and

$$z_k = \psi(kh), \qquad k = 0, \pm 1, \ldots. \tag{2.16}$$

A direct application of the methodology in [7] to (1.1) does not lead to a symmetric discrete system. To symmetrize the discrete system, the change of variable

$$w(t) = (\sqrt{\phi'}\, u) \circ \psi(t) \tag{2.17}$$

is made in (1.1). The resulting change of variable does not introduce a first derivative term in the transformed equation

$$\begin{aligned} Lw(t) &= -w''(t) + \{\gamma_q(t)\}\, w(t) \\ &= \lambda \rho(\psi(t))(\psi'(t))^2\, w(t), \\ &\lim_{t \to \pm\infty} w(t) = 0, \end{aligned} \tag{2.18}$$

where

$$\begin{aligned} \gamma_q(t) = &-(\psi'(t))^{1/2} \frac{d}{dt}\left\{\frac{1}{\psi'(t)} \frac{d}{dt}((\psi'(t))^{1/2})\right\} \\ &+ [\psi'(t)]^2\, q(\psi(t)). \end{aligned} \tag{2.19}$$

If (2.14) is an assumed approximate solution of (2.18) then substitution of the former in the latter yields the equations

$$\begin{aligned} LC_M(w, h)(jh) = &\frac{-1}{h^2} \sum_{k=-M}^{M} \delta_{jk}^{(2)} w(kh) + \gamma_q(jh)\, w(jh) \\ &= \lambda(\rho(\psi(jh)))(\psi'(jh))^2\, w(jh), \qquad -M \leqslant j \leqslant M, \end{aligned} \tag{2.20}$$

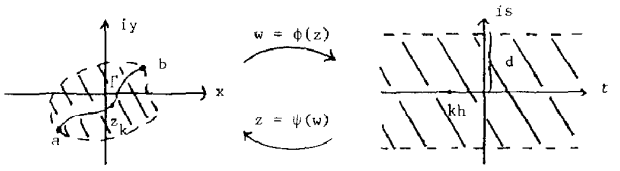


FIG. 1. The map $\phi$ and its inverse $\psi$.

where

$$\delta_{jk}^{(2)} \equiv h^2 \frac{d^2}{dt^2} S(k, h)(t) \Big|_{t=jh} = \begin{cases} \dfrac{-\pi^2}{3}, & j = k \\ \dfrac{(-2)(-1)^{j-k}}{(j-k)^2}, & j \neq k. \end{cases} \tag{2.21}$$

The collocation scheme defined by (2.20) has the more compact matrix representation

$$\overline{LC_M}(w, h) = A\bar{w} = \lambda D(\rho(\psi')^2)\,\bar{w}, \tag{2.22}$$

where

$$A = \frac{-1}{h^2} I^{(2)} + D(\gamma_q). \tag{2.23}$$

In (2.23) the matrix $I^{(2)}$ is the $m \times m$ $(m = 2M + 1)$ matrix whose $j, k$th entry is given by (2.21). The matrix $D(f)$ is the $m \times m$ diagonal matrix whose diagonal entries are $f(x_j)$, $j = -M, \ldots, 0, \ldots, M$ and $x_j = \psi(jh)$ in (2.16). The $m$-vector $\bar{w}$ in (2.22) is $(w(-Mh), w((-M+1)h), \ldots, w(0), \ldots, w(Mh))^{\mathrm{T}}$.

It has been shown in [12] that the spectrum of $-I^{(2)}$ is contained in the interval $(0, \pi^2)$ independently of $M$. Hence if $D(\gamma_q)$ has nonnegative entries the matrix $A$ in (2.23) is a symmetric positive definite matrix. The expression in (2.19) for arbitrary $\psi$ and $q$ is a bit unwieldy and for the remainder of this section it will be assumed that

$$\gamma_q(t) \geq (\delta(q, \psi, h))^{-1} = \delta^{-1} > 0, \qquad t \in (-\infty, \infty). \tag{2.24}$$

The quantity defined in (2.24) is explicitly worked out in Section III. It is pointed out there that for the maps $\psi$ of this paper and nonnegative $q$ that there is always a $\delta$ (depending only on $q$) so that (2.24) holds. Note that the inequality in (2.24) implies that

$$\alpha_{-M} \equiv \min_{\alpha_j \in \sigma(A)} \{\alpha_j\} \geq \delta^{-1}. \tag{2.25}$$

For the development of the remainder of this section the symmetry of $A$ in (2.23) and the positive definiteness of $D(\rho(\psi')^2)$ play a fundamental role. These two properties guarantee that the matrix eigenvalue problem (2.22) form a definite pencil [9]. This not only guarantees the existence of the matrix $Z$ in (2.31), but eliminates any worry over possibly singular pencils or ill-disposed eigenvalues.

To proceed with the development of the approximate eigenvalue problem assume that $\lambda_0$ and $w_0(t)$ is an eigenpair of (2.18) where $w_0$ is normalized by

$$\int_{-\infty}^{\infty} w_0^2(t)\,\rho(\psi(t))[\psi'(t)]^2\,dt = 1. \tag{2.26}$$

Note that with the change of variable defined by (2.17) the equality in (2.26) is equivalent to the assumption that

$$\int_a^b u_0^2(x)\,\rho(x)\,dx = 1. \tag{2.27}$$

Upon substituting $w_0$ in (2.18) and evaluating at $t = jh$ $(-M \leqslant j \leqslant M)$ it follows that

$$\overline{Lw}_0 = \lambda_0 D(\rho(\psi')^2)\,\bar{w}_0. \tag{2.28}$$

Subtracting (2.28) from (2.22) yields the equalities

$$\begin{aligned}\overline{\Delta w}_0 &= \overline{LC}_M(w_0, h) - \overline{Lw}_0 \\ &= (A - \lambda_0 \mathscr{D}^2)\,\bar{w}_0,\end{aligned} \tag{2.29}$$

where

$$\mathscr{D} = D(\sqrt{\rho}\,\psi'). \tag{2.30}$$

Since $A$ and $\mathscr{D}^2$ are positive definite there are eigenvectors $\bar{z}_i$ and positive eigenvalues $\mu_i \leqslant \mu_j$ $(-M \leqslant i < j \leqslant M)$ so that

$$Z^T A Z = \begin{pmatrix} \mu_{-M} & & & & \\ & \ddots & & \bigcirc & \\ & & \mu_0 & & \\ & \bigcirc & & \ddots & \\ & & & & \mu_M \end{pmatrix}, \tag{2.31}$$

$$Z^T \mathscr{D}^2 Z = I,$$

and

$$A\bar{z}_i = \mu_i \mathscr{D}^2 \bar{z}_i, \qquad i = -M, \ldots, M. \tag{2.32}$$

The independence of the $\{\bar{z}_i\}_{i=-M}^{M}$ imply that there are constants $\beta_i$ so that

$$\bar{w}_0 = \sum_{i=-M}^{M} \beta_i \bar{z}_i. \tag{2.33}$$

Substituting (2.33) in the right-hand side of (2.29) yields the equality

$$\overline{\Delta w}_0 = \sum_{i=-M}^{M} \beta_i(\mu_i - \lambda_0)\mathscr{D}^2 \bar{z}_i. \tag{2.34}$$

Taking the inner product of the eigenvector $\bar{z}_p$ with each side of (2.34) shows that

$$\bar{z}_p^T\,\overline{\Delta w}_0 = \beta_p(\mu_p - \lambda_0), \qquad p = -M, \ldots, M. \tag{2.35}$$

Applying $\mathscr{D}^2$ to both sides of (2.33) and taking the inner product of this result with $\bar{w}_0$ leads, upon using (2.32), to the identity

$$\|\mathscr{D}\bar{w}_0\|_2^2 = \sum_{i=-M}^{M} \beta_i^2 \leqslant \beta_p^2(2M+1), \tag{2.36}$$

where

$$|\beta_p| \equiv \max_{-M \leqslant i \leqslant M} \{|\beta_i|\}. \tag{2.37}$$

Assume that the eigenfunction $w_0$ of (2.18) is an element of $B(S_d)$ and that $w_0$ satisfies the growth condition in (2.9). Application of the trapezoidal quadrature rule to the left-hand side of (2.26) shows that

$$\begin{aligned} 1 &= h \sum_{j=-M}^{M} w_0^2(jh)\, \rho(\psi(jh))[\psi'(jh)]^2 + \varepsilon(w_0, M) \\ &= h\, \|\mathscr{D}\bar{w}_0\|_2^2 + \varepsilon(w_0, M). \end{aligned} \tag{2.38}$$

The assumptions on $w_0$ and [13] guarantee that $|\varepsilon(w_0, M)/h| \to 0$ as $M \to \infty$ so that, for sufficiently large $M$, $|\varepsilon(w_0, M)/h| \leqslant 1/(2h)$. Hence $\|\mathscr{D}\bar{w}_0\|_2^2 \geqslant 1/(2h)$ which, when combined with (2.36), yields

$$|\beta_p| \geqslant (2(2M+1)\, h)^{-1/2}. \tag{2.39}$$

The inequality (2.24) shows that

$$\begin{aligned} \delta^{-1} &\leqslant \min_{\alpha_j \in \sigma(A)} \{\alpha_j\} \equiv \alpha_{-M} \\ &= \min_{\bar{x}^T\bar{x}} \left\{ \frac{\bar{x}^T A \bar{x}}{\bar{x}^T \bar{x}} \right\} \\ &\leqslant \bar{z}_j^T A \bar{z}_j / \|\bar{z}_j\|_2^2. \end{aligned} \tag{2.40}$$

The equality in (2.31) shows that $\bar{z}_j^T A \bar{z}_j = \mu_j$ which when substituted in the right-hand side of (2.40) leads to the estimate

$$\|\bar{z}_j\|_2^2 \leqslant \delta \mu_j. \tag{2.41}$$

Assume that $\lambda_0$ and $w_0$ is an eigenpair of (2.18). Let $p$ denote the index defined in (2.37) and assume

$$|\mu_p - \lambda_0| \leqslant \lambda_0. \tag{2.42}$$

The latter condition will be shown in what follows to hold for all sufficiently large $M$. If $\theta_p$ is the angle between the vectors $\bar{z}_p$ and $\overline{A w_0}$ then upon taking absolute values in (2.35) and expanding the inner product on the left-hand side yields

$$|\mu_p - \lambda_0| = \frac{\|\bar{z}_p\|_2\, \|\overline{A w_0}\|_2\, |\cos(\theta_p)|}{|\beta_p|}. \tag{2.43}$$

The inequality in (2.42) shows that

$$\mu_p = \mu_p - \lambda_0 + \lambda_0 \leqslant |\mu_p - \lambda_0| + \lambda_0 \leqslant 2\lambda_0 \tag{2.44}$$

which when substituted in (2.41) gives

$$\|\bar{z}_p\|_2^2 \leqslant 2\lambda_0\, \delta. \tag{2.45}$$

Replacing $\|\bar{z}_p\|_2$ and $|\beta_p|$ in (2.43) by the right-hand sides of (2.45) and (2.39), respectively, leads to

$$|\mu_p - \lambda_0| \leqslant 2\{((2M+1)\,h)^{1/2}\,|\cos(\theta_p)|\}\,\sqrt{\delta\lambda_0}\,\|\overline{\Delta w}_0\|_2. \tag{2.46}$$

A more convenient form for the error in (2.46) may be obtained by a short computation using (2.29) and the interpolatory property $S(k, h)(jh) = \delta_{jk}$. This leads to

$$\begin{aligned} |\Delta w_0(jh)| &= |LC_M(w_0, h)(jh) - Lw_0(jh)| \\ &= \left| \frac{d^2}{dt^2}\, C_M(w_0, h)(jh) - \frac{d^2}{dt^2}\, w_0(jh) \right|. \end{aligned} \tag{2.47}$$

Combining this identity with (2.13) shows that

$$\|\overline{\Delta w}_0\|_2 \leqslant KM^{5/4} \exp(-(\pi d\alpha M)^{1/2}). \tag{2.48}$$

Finally, the substitutions $h = (\pi d/\alpha M)^{1/2}$, $|\cos\theta_p| \leqslant 1$ and the right-hand side of (2.48) for $\|\overline{\Delta w}_0\|_2$ in (2.46) yield the error estimate

$$|\mu_p - \lambda_0| \leqslant K\sqrt{\delta\lambda_0}\, M^{3/2} \exp -(\pi d\alpha M)^{1/2}. \tag{2.49}$$

Note in the case complimentary to (2.42),

$$|\mu_p - \lambda_0| > \lambda_0, \tag{2.50}$$

that the inequality (2.43) is replaced by

$$\mu_p \leqslant 2\,|\mu_p - \lambda|. \tag{2.51}$$

In this case the right-hand side of (2.45) is replaced by $2\delta\,|\mu_p - \lambda_0|$. Hence the inequality in (2.42) is the same as listed if $\lambda_0^{1/2}$ on the right-hand side of (2.49) is replaced by $|\mu_p - \lambda_0|^{1/2}$. With the replacement of the previous sentence, (2.49) remains valid. Hence $|\mu_p - \lambda_0| \to 0$ as $M \to \infty$. While it is possible that (2.50) is valid for some values of $M$, as $M$ increases the inequality (2.42) takes over. For the remainder of this paper it will be assumed that (2.42) is valid. Indeed, in all of the examples of the next section the inequality (2.42) is valid for all $M \geqslant 2$.

The preceding development is summarized as follows. If the change of variable

$$w(t) = (\sqrt{\phi'}\, u) \circ \psi(t)$$

is made in the Sturm–Liouville problem

$$-u''(x)+q(x)\,u(x)=\lambda\rho(x)\,u(x), \qquad a<x<b,$$
$$u(a)=u(b)=0$$

the transformed problem takes the form

$$-w''(t)+\gamma_q(t)\,w(t)=\lambda\rho(\psi(t))(\psi'(t))^2\,w(t), \qquad -\infty<t<\infty,$$
$$\lim_{t\to\pm\infty}(w(t))=0,$$

where

$$\gamma_q(t)=-(\psi'(t))^{1/2}\frac{d}{dt}\left\{\frac{1}{\psi'(t)}\frac{d}{dt}(((\psi'(t))^{1/2}))\right\}+[\psi'(t)]^2\,q(\psi(t))$$

and the map $\psi=\phi^{-1}$ is characterized in Definition 2.1. If the transformed problem is approximated by collocating the sinc expansion

$$C_{M,N}(w,h)(t)=\sum_{k=-M}^{N} w(kh)\,S(k,h)(t)$$

at the trapezoidal nodes $t_i=ih$, $-M\leqslant i\leqslant N$, there results the generalized eigenvalue problem

$$\{-1/h^2I^{(2)}+D(\gamma_q)\}\,\bar{z}_i=\mu_i D(\rho(\psi')^2)\,\bar{z}_i, \qquad -M\leqslant i\leqslant N$$

for the approximation of the eigenvalues $\lambda$ of the continuous Sturm–Liouville problem by $\mu_i$.

THEOREM 2.1. *Let $\lambda_0$, $w_0$ be an eigenpair of the transformed differential equation. Assume that $w_0\in B(S_d)$ ($w_0$ satisfies (2.4), (2.5)) and there are positive constants $\alpha$, $\beta$, and $C$ so that*

$$|w(t)|\leqslant C\begin{cases}\exp(\alpha t), & t\in(-\infty,0]\\ \exp(-\beta t), & t\in(0,\infty).\end{cases}$$

*If there is a constant $\delta>0$ so that $|\gamma_q(t)|\geqslant\delta^{-1}$ and the selections $h=(\pi d/\alpha M)^{1/2}$ and $N=[\![(\alpha/\beta)\,M]\!]$ are made then there is an eigenvalue $\mu_p$ of the generalized eigenvalue problem satisfying*

$$|\mu_p-\lambda_0|\leqslant K\sqrt{\delta\lambda_0}\,M^{3/2}\exp(-(\pi d\alpha M)^{1/2}).$$

Before turning to the numerical method based on the matrix system (2.32) note that the matrix eigenvalue problem has $2M+1$ eigenvalues $\mu_i$. The continuous problem has, in general, an infinite number of eigenvalues $\{\lambda_i\}_{i=0}^{\infty}$. The inequality

(2.46) holds for arbitrary $\lambda_0$. Note that due to the factor $\sqrt{\lambda_0}$ on the right-hand side of (2.46) one would expect that the spectral values at the lower end of the spectrum to be more accurately computed than the larger spactral values. This is borne out in all of the examples of the next section.

## III. Numerical Implementation

The implementation of the numerical scheme using the matrix system (2.22) with the parameter selections given by (2.11) and (2.12) is developed in this section. Since Section II was not specific with regard to the functions $q$ and $\rho$ in (1.1) (with the exception of the nonnegativity assumption), this section, by way of examples, will indicate extensions in the application of Theorem 2.1. Indeed the motivation for the selection of the examples is twofold: (a) to highlight the aforementioned extensions, and (b) to give the user certain "rules of thumb" guides in the selection of the parameters needed to implement the method. The latter is explored in depth for the $(0, \infty)$ boundary value problem since there are two conformal maps which may be used for this case. As such, the section conveniently separates itself into the two cases: the interval $(a, b)$ is finite and the interval $(a, b) = (0, \infty)$.

The result of Theorem 2.1 is based on the assumed approximate solution (2.14) of the transformed boundary value problem (2.18). In terms of the given boundary value problem

$$\begin{gathered} Lu = -u''(x) + q(x)\, u(x) = \lambda \rho(x)\, u(x), \qquad a < x < b, \\ u(a) = u(b) = 0 \end{gathered} \tag{3.1}$$

the assumed approximate solution is

$$C_{M,N}(u, h)(x) = \sum_{k=-M}^{N} (\phi'(x_k))^{1/2}\, u(x_k)\, S(k, h) \circ \phi(x). \tag{3.2}$$

The identity in (3.2) is obtained from (2.14) via $t = \phi(x)$ from Definition 2.1, $x_k = \psi(kh)$ in (2.16) and (2.17). In terms of $\phi$ the quantity $\gamma_q(t) = \gamma_q(\phi(x))$ in (2.19) takes the form

$$\gamma_q(x) = -(\phi(x))^{-3/2}((\phi'(x))^{-1/2})'' + (\phi'(x))^{-2}\, q(x). \tag{3.3}$$

The coefficient matrix $A$ in (2.22) (dimension $m \times m$ $(m = M + N + 1)$) is defined in (2.23) and has been included in Fig. 2. The second line of this figure is the generalized eigenvalue problem whose eigenvalues are approximate eigenvalues of (3.1). The formula required for the construction of the matrix $A$ for the maps $\phi_i$ on $(a, b)$ $(i = 1, 2, 3)$ are also summarized in Fig. 2. A glance at the fourth column of the figure shows that for the first two maps the quantity $\gamma_q(x)$ in (3.3) is bounded below by $\frac{1}{4}$. Hence, for these two maps, the quantity $\delta$ in (2.24) and (2.49) may be

$$A = \frac{-1}{h^2} I^{(2)} + D\left(\frac{-1}{(\phi')^{3/2}}(1/\sqrt{\phi'})'' + \frac{q}{(\phi')^2}\right),$$

$$A\bar{z} = \mu \mathscr{L}^2 \bar{z}, \qquad \mathscr{L} = D(\sqrt{\rho}/\phi').$$

| Interval | $\phi$ | $(\phi')^{-1}$ | $-(\phi')^{3/2}((\phi')^{-1/2})''$ | $x_k$ |
|---|---|---|---|---|
| $(a, b)$ | $\phi_1(x) = \log\left(\frac{x-a}{b-x}\right)$ | $\frac{(x-a)(b-x)}{b-a}$ | $\frac{1}{4}$ | $\frac{be^{kh}+a}{e^{kh}+1}$ |
| $(0, \infty)$ | $\phi_2(x) = \log(x)$ | $x$ | $\frac{1}{4}$ | $e^{kh}$ |
| $(0, \infty)$ | $\phi_3(x) = \log(\sinh(x))$ | $\tanh(x)$ | $\frac{4\cosh^2 x - 3}{4\cosh^4 x}$ | $\log[e^{kh} + \sqrt{e^{2kh}+1}]$ |

FIG. 2. Discrete system used to compute the approximate eigenvalues for (3.1).

replaced by four. In problems where $q(x)$ is not nonnegative on $(a, b)$ the method of Section II may still be applicable as indicated by Example 3.3. For the map $\phi_3(x) = \log(\sinh(x))$ the quantity

$$\gamma_q(x) = \frac{4\cosh^2(x) - 3}{\cosh^4(x)} + (\tanh^2(x))\, q(x)$$

is problem dependent with respect to being bounded away from zero. However, if $\liminf_{x \to \infty} q(x) \neq 0$, then there is a positive $\delta$ so that (2.24) is satisfied. Indeed, in Examples 3.5 and 3.6 where the map $\phi_3$ is used the $\delta$ in (2.24) may be taken to be 4 and $\frac{1}{2}$, respectively.

The assumed bound on the transformed solution $w$ in (2.9), using the change of variable (2.17), takes the form

$$|\sqrt{\phi'}(x)\, u(x)| \leqslant C \begin{cases} \exp(-\alpha\, |\phi(x)|), & x \in \Gamma_a \\ \exp(-\beta\, |\phi(x)|), & x \in \Gamma_b, \end{cases} \tag{3.5}$$

where

$$\Gamma_a = \{\psi(t) : t \in (-\infty, 0]\}, \qquad \Gamma_b = \{\psi(t) : t \in (0, \infty)\}. \tag{3.6}$$

The parameter selections

$$h = (\pi d/\alpha M)^{1/2} \tag{3.7}$$

and

$$N = \left\lfloor \frac{\alpha}{\beta} M \right\rfloor \tag{3.8}$$

are, in general, what are used for the construction of $A$ in Fig. 2. The quantity $\alpha$ in (3.5) is determined as follows. Assume that (3.1) has at worst a regular singular point at $a$, so that

$$\lim_{x \to a^+} (x-a)^2 h(x) = h_a, \tag{3.9}$$

where $h$ is $q$ or $\rho$. The indicial equation for (3.1) reads

$$s(s-1) - (q_a + \rho_a) = 0 \tag{3.10}$$

which, since $q_a + \rho_a > 0$, has one positive root $s_+$ and one negative root $s_-$. The boundary condition $u(a) = 0$ eliminates the root $s_-$ and the selection

$$\alpha = s_+ - \tfrac{1}{2} \tag{3.11}$$

is used in (3.7).

If $b$ is finite the procedure outlined in (3.9)–(3.11) is used for the determination of $\beta$ in (3.5). At this point it is convenient to distinguish two cases: $b$ is positive infinity, and $b$ is finite. In the latter case a short computation, using the map $\phi_1$ in Fig. 2, shows that the inequality (3.5) is equivalent to

$$|u(x)| \leqslant C_1 \begin{cases} (x-a)^{\alpha+1/2}, & x \in \Gamma_a \\ (b-x)^{\beta+1/2}, & x \in \Gamma_b. \end{cases} \tag{3.12}$$

In (3.12), reference to (3.6), shows that $\Gamma_a = (a, (a+b)/2]$ and $\Gamma_b = ((a+b)/2, b)$.

In each of the first three examples the interval is finite. The exact selections of the parameters (3.7), (3.8), and (3.11) are included in the text of each example. The first two examples are regular Sturm–Liouville problems and the third example is a singular Sturm–Liouville problem. For all of these finite interval examples the value $d = \pi/2$ is used in (3.7), i.e., the domain $D_{\pi/2}$ for $\phi_1$ in Fig. 3 is a disc.

In the displays for every example the notation $.xxx - C$ is $.xxx \times 10^{-C}$. The quantity in the second line of each display

$$\begin{aligned} \text{AER} &= \text{Asymptotic Error Rate} \\ &\equiv \exp(-(\pi d \alpha M)^{1/2}), \end{aligned} \tag{3.13}$$

is taken from the right-hand side of (2.49). In a number of the displays it will be noted that the absolute error $|\mu_p - \lambda_p|$ is smaller than the asymptotic rate in (3.13). A partial explanation can be found if it is recalled that the right-hand side of (2.49) is obtained by replacing $|\cos \theta_p|$ in (2.46) by one ($\theta_p$ is the angle between the eigenvector $\bar{z}_p$ and the error vector $\overline{\Delta w}_0$). It appears (numerically) that the latter two vectors approach orthogonality. However, for an arbitrary problem these authors have not been able to establish a rate of convergence for $|\cos \theta_p|$ ($\to 0$) as a function of $h$. To exemplify this remark the quantity

$$Q = M^{3/2} |\cos \theta_p| \exp(-(\pi d \alpha M)^{1/2})$$

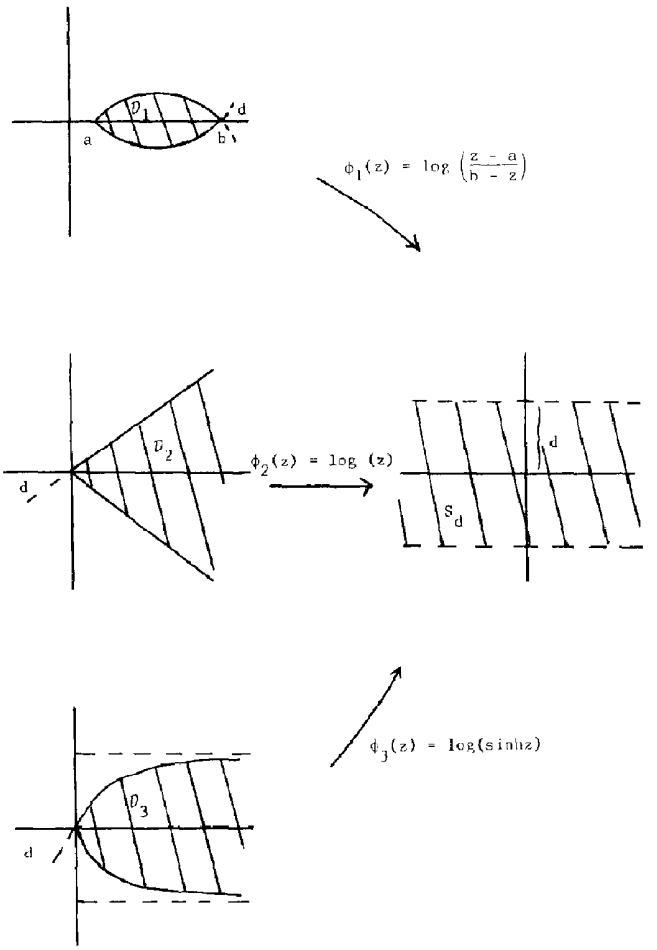


FIG. 3. The domains $\mathcal{D}_i$ and maps $\phi_i$.

is listed under the AER heading in both of the Examples 3.4 and 3.7. These two examples indicate that the rate at which $|\cos\theta_p|$ approaches zero may be quite different.

EXAMPLE 3.1. (Fourier) $-u''(x) = \lambda u(x)$, $u(0) = u(\pi) = 0$.

Here (3.12) is satisfied for $\alpha = \beta = \frac{1}{2}$ so that (3.7) is given by $h = \pi/\sqrt{M}$ and $N = M$ in (3.8). The computed eigenvalues $\mu_p$ are obtained (see Table I) from the solution of the $m \times m$ ($m = 2M + 1$) system ($a = 0$, $b = \pi$ for $\phi_1$ in Fig. 2),

$$A\bar{z}_p = \left(\frac{-1}{h^2} I^{(2)} + D\left(\frac{1}{4}\right)\right)\bar{z}_p = \mu_p D\left(\frac{x_k^2(\pi - x_k^2)}{\pi^2}\right)\bar{z}_p,$$

$$x_k = \pi e^{kh}/(e^{kh} + 1).$$

TABLE I

| True eigenvalues | 4 | 8 | 16 | 24 | $=M$ |
|---|---|---|---|---|---|
| $\lambda_p$ | 0.432–1 | 0.118–1 | 0.187–2 | 0.455–3 | = AER |
| | | | $\lvert\mu_p-\lambda_p\rvert$ | | |
| 1 | 0.182–1 | 0.659–3 | 0.109–5 | 0.370–6 | |
| 4 | — | 0.797–1 | 0.173–2 | 0.623–4 | |
| 9 | — | — | 0.716–1 | 0.469–2 | |
| 16 | — | — | — | 0.940–1 | |

EXAMPLE 3.2. $-u''(x)+(\cos^2 x)\,u(x)=\lambda u(x)$, Mathieu $u(0)=u(\pi)=0$.

As in the last example $\alpha=\beta=\frac{1}{2}$, $h=\pi/\sqrt{M}$ and $N=M$. The errors listed in Table II were computed using the eigenvalues listed for Mathieu's equation in [1].

EXAMPLE 3.3. (Tschebyscheff) $-u''(x)+(-3/4)(1-x^2)^{-2}\,u(x)=\lambda(1-x^2)^{-1}\,u(x)$, $u(-1)=u(1)=0$.

In this example $q(x)=-\frac{3}{4}(1-x^2)^{-1}<0$ on $(-1,1)$ so that the development leading to Theorem 2.1 is not applicable. However, the only role played by the non-negativity assumption $q(x)\geqslant 0$ in Section II was in establishing the inequality (2.25). For the present example, reference to (3.3) and Fig. 2 shows that

$$\gamma_q(x)=\tfrac{1}{4}+\tfrac{1}{4}(1-x^2)^2\,q(x)=\tfrac{1}{16}.$$

Hence if $\delta$ in (2.25) is replaced by 16 the remainder of Section II remains intact and Theorem 2.1 is applicable to this example. Indeed, for any finite interval example in which

$$\liminf_{x\in(a,b)}\left\{\frac{q(x)}{(\phi_1'(x))^2}\right\}>-\frac{1}{4}$$

the convergence rate given by the right-hand side of (2.49) applies. Equation (3.9) gives $q_{-1}=-\frac{3}{16}$ and $\rho_{-1}=0$ so that (3.10) and (3.11) give $\alpha=\frac{1}{4}$. The same

TABLE II

| True eigenvalues | 4 | 8 | 16 | 24 | $=M$ |
|---|---|---|---|---|---|
| $\lambda_p$ | 0.432–1 | 0.118–1 | 0.187–2 | 0.455–3 | = AER |
| | | | $\lvert\mu_p-\lambda_p\rvert$ | | |
| 1.24242 | 0.106–0 | 0.144–1 | 0.414–3 | 0.140–4 | |
| 4.49479 | — | 0.151–0 | 0.697–2 | 0.481–3 | |
| 9.50366 | — | — | 0.109–0 | 0.985–2 | |
| 16.50208 | — | — | — | 0.124–0 | |

procedure yields $\beta = \frac{1}{4}$ so that $h = 2\pi/\sqrt{M}$ and $N = M$ in (3.7) and (3.8), respectively. Note that these selections give the correct behavior of the eigensolutions (see Table III)

$$u_{\lambda_p}(x) = (1 - x^2)^{3/4} U_p(x),$$
$$\lambda_p = p(p+2) + 3/4, \qquad p = 0, 1, 2, \ldots, \tag{3.14}$$

where $U_p$ is the $p$th Tschebyscheff polynomial of the second kind. For this example the discrete system in Fig. 2 takes the form ($a = -1$, $b = -1$ for $\phi_1$ in Fig. 2):

$$A\bar{z}_p = \left(\frac{-1}{h^2} I^{(2)} + D\left(\frac{1}{16}\right)\right) \bar{z}_p = \mu_p D\left(\frac{1 - x_k^2}{4}\right) \bar{z}_p,$$
$$x_k = (e^{kh} - 1)/(e^{kh} + 1).$$

In the case of problems (3.1) on $(0, \infty)$ the inequality (3.5) is equivalent to

$$|u(x)| \leqslant C_1 \begin{cases} x^{\alpha + 1/2}, & x \in \Gamma_0 = (0, 1] \\ x^{-\beta + 1/2}, & x \in \Gamma_\infty = (1, \infty) \end{cases} \tag{3.15}$$

for the map $\phi_2(x) = \log(x)$. For the map $\phi_3(x) = \log(\sinh(x))$ one finds

$$|u(x)| \leqslant C_1 \begin{cases} x^{\alpha + 1/2}, & x \in \Gamma_0 = (0, \log(1 + \sqrt{2})] \\ e^{-\beta x}, & x \in \Gamma_\infty = (\log(1 + \sqrt{2}), \infty). \end{cases} \tag{3.16}$$

These inequalities provide the first indication of how it is decided on which $(0, \infty)$ map is to be used. If (3.1) has eigensolutions that decay exponentially at $\infty$, i.e., as $x$ tends to infinity

$$u(x) \sim \exp(-\gamma x), \qquad \gamma > 0, \tag{3.17}$$

then the second inequality in (3.15) and (3.16) is satisfied on $\Gamma_\infty$. However, since (3.15) requires only the algebraic decay of the solution on $\Gamma_\infty$, it was shown in [6] that it is advantageous to replace (3.8) by the choice

$$N = \left[\!\left[\frac{1}{h} \log\left(\frac{\alpha}{\gamma} Mh\right) + 1\right]\!\right] \tag{3.18}$$

TABLE III

| True eigenvalues | 4 | 8 | 16 | 24 | $= M$ |
|---|---|---|---|---|---|
| $\lambda_p$ | 0.108–0 | 0.432–1 | 0.118–1 | 0.433–2 | = AER |
| | | | $\lvert\mu_p - \lambda_p\rvert$ | | |
| $\frac{3}{4}$ | 0.521–0 | 0.181–1 | 0.210–3 | 0.319–4 | |
| $\frac{15}{4}$ | — | 0.536–1 | 0.187–2 | 0.170–3 | |
| $\frac{35}{4}$ | — | — | 0.321–1 | 0.183–2 | |
| $\frac{63}{4}$ | — | — | — | 0.381–1 | |

when using map $\phi_2(x) = \log(x)$. This selection reduces the dimension of $A$ in Fig. 2 and consequently yields a smaller generalized eigenvalue problem to solve for the $\mu_p$ in $A\xi_p = \mu_p \mathscr{D}^2 \xi_p$. Example 3.4 is included to demonstrate the selection (3.18) in the case of Laguerre's boundary value problem.

A second criteria employed in differentiating whether to use the map $\phi_2(x)$ or $\phi_3(x)$ is predicated on the behavior of the solution $u$ of (3.1) in the right half-plane. If the coefficients $q$ and $\rho$ in (3.1) are analytic in a sector of the right half-plane then the solution is analytic in the sector [8, p. 145] and the map $\phi_2$ is in general used. If it is not possible to prove the analyticity of the solution of (3.1) in a sector or if the solution has singularities in the right half plane that are "near" the positive half line then the map $\phi_3$ is used. This latter case is discussed in more detail in the computation of the eigenvalues for the Schrodinger equation with a Wood–Saxon potential in Example 3.5. Example 3.6 exhibits a boundary value problem where either of the maps $\phi_i$ $(i = 2, 3)$ are applicable. However, due to the assumed bound in (2.6), the map $\phi_3$ yields a somewhat more computationally efficient scheme.

The selection of $h$ for all of the $(0, \infty)$ examples is given by (3.7) where $\alpha$, as in the finite interval case, is obtained from (3.10) and (3.11). Finally, the selection of $N$ is given by (3.8) except, as in Example 3.4, when the remarks following (3.17) are applicable. The number $\beta$ in (3.8) is most conveniently ascertained by using the WKB approximation [8, p. 191]. The final Example 3.7 is less typical then the preceding three. It is included to exhibit a case where the rate of convergence given by the right-hand side of (2.49) obtains for the map $\phi_2$ but, due to (3.16), cannot be obtained for the map $\phi_3$.

EXAMPLE 3.4. (Laguerre) $-u''(x) + [(x^2+3)/4x^2]\, u(x) = \lambda(1/2x)\, u(x)$, $u(0) = u(\infty) = 0$.

In this case, with $a = 0$ in (3.9), Eq. (3.10) becomes $s(s-1) - 3/4 = 0$ so that $s_+ = \frac{3}{2}$ and from (3.11) $\alpha = 1$. The solutions are analytic in the right half-plane so with $d = \pi/2$ in (3.7) the parameter $h = \pi/\sqrt{2M}$. The WKB approximation yields for constant $\eta$,

$$u_i(x) \sim \eta \exp(-x/2), \qquad x \to +\infty \tag{3.19}$$

so that (3.15) is satisfied if $\beta > 0$ and (3.16) is satisfied with $\beta = \frac{1}{2}$. In light of the comments following (3.17), the selection (3.18), i.e.,

$$N = \left\lceil \frac{1}{h} \log(2Mh) + 1 \right\rceil \tag{3.20}$$

is used with the map $\phi_2(x) = \log(x)$. It should be pointed out that the errors listed in Table IV would be the same for the map $\phi_3$ if (3.20) is replaced by (3.8) $(N = 2M)$. Note, however, in the latter case that the dimension of $A$ in Fig. 1 would

TABLE IV

| True eigenvalues | 4 | 8 | 16 | 24 | $=M$ |
|---|---|---|---|---|---|
| $\lambda_p$ | 0.118–1 | 0.187–2 | 0.138–3 | 0.188–4 | = AER |
| | 0.244–1 | 0.197–2 | 0.879–4 | 0.376–5 | $=Q$ |
| | | | $\lvert\mu_p-\lambda_p\rvert$ | | |
| 3 | 0.242–1 | 0.111–2 | 0.283–4 | 0.868–6 | |
| 5 | — | 0.123–1 | 0.101–2 | 0.485–4 | |
| 7 | — | — | 0.172–1 | 0.124–2 | |
| 9 | — | — | — | 0.108–1 | |

be $m \times m$ where $m = 13, 25, 49, 73$ ($M = 4, 8, 16, 24$). This is to be contrasted with the size of $A$ in

$$A\bar{z}_p = \left\{\frac{-1}{h^2} I^2 + D\left(\frac{1}{4} + \frac{x_k(x_k^2+3)}{4}\right)\right\} \bar{z}_p = \mu_p D\left(\frac{x_k}{2}\right) \bar{z}_p,$$

$$x_k = \exp(kh)$$

which is $m \times m$ ($m = 7, 13, 23, 32$ ($m = M+N+1$, $M = 4, 8, 16, 24$)). The true eigensolutions for this example are

$$u_{\lambda_p}(x) = x^{3/2} e^{-x/2} \left\{\frac{e^x}{p! x^2} \frac{d^p}{dx^p} (x^{p+2} e^{-x})\right\},$$

$$\lambda_p = 2p + 3, \qquad p = 0, 1, \ldots.$$

As indicated in the paragraph preceeding Example 4.1, the third row in Table IV is the quantity $Q = M^{3/2} |\cos \theta_p| \exp(-(\pi d \alpha M)^{1/2})$.

EXAMPLE 3.5. (Wood–Saxon) $-u''(x) + u(x) = \lambda(1 + e^{(x-r)/\varepsilon})^{-1} u(x)$, $u(0) = u(\infty) = 0$.

Equation (3.10) with $q_0 = \rho_0 = 0$ gives $s_+ = 1$ so that $\alpha = \frac{1}{2}$. Due to the pole of $\rho(x)$ at $r + \varepsilon\pi i$ the largest sector in which the solution can be guaranteed to be analytic has $d = \mathrm{Tan}^{-1}(\varepsilon\pi/r)$. For comparison purposes ([7] and [10]) the

TABLE V

| True eigenvalues | 4 | 8 | 16 | 24 | $=M$ |
|---|---|---|---|---|---|
| $\lambda_p$ | 0.432–1 | 0.118–1 | 0.178–2 | 0.454–3 | = AER |
| 1.424333 | 1.427127 | 1.424484 | 1.424335 | 1.424333 | |
| $\lambda_2$ | — | 2.447301 | 2.444763 | 2.444707 | |
| $\lambda_3$ | — | — | 3.972775 | 3.972332 | |
| $\lambda_4$ | — | — | — | 5.993260 | |

parameters are $r = 5.086855$ and $\varepsilon = 0.929853$. Hence if the map $\phi_2(x)$ is selected $d$ must be selected smaller than (approximately) $\pi/6$. For the domain of $\phi_3$ in Fig. 3 there is no such restriction on $d$ and an inspection of the right-hand side of (2.46) shows a faster convergence rate for larger values of $d$. The correct asymptotic behavior of the solution is found in [4, p. 164]

$$u(x) \sim \exp(-(x-r)/\varepsilon), \qquad x \to \infty.$$

Hence, one may select $\beta = 1$ in (3.16), so with $\alpha = 2$ Eqs. (3.7) and (3.8) give $h = \pi/\sqrt{M}$ and $2N = M$, respectively. The first true eigenvalue listed in Table V has been computed in [7] and [10]. The numbers listed in Table V are computed from matrix system

$$A\bar{z}_p = \left\{ \frac{-1}{h^2} I^2 + D\left( \frac{4\cosh^2 x_k - 3}{4\cosh^4 x_k} + \tanh^2 x_k \right) \right\} \bar{z}_p$$

$$= \mu_p D \left( \frac{\tanh^2 x_k}{1 + e^{(x_k - r)/\varepsilon}} \right) \bar{z}_p,$$

$$x_k = \log(e^{kh} + \sqrt{e^{2kh} + 1}).$$

EXAMPLE 3.6. (Harmonic Oscillator) $-u''(x) + (x^2 + 2x^{-2})\, u(x) = \lambda u(x)$, $u(0) = u(\infty) = 0$.

Equation (3.10) with $q_0 = 2$ and $\rho_0 = 0$ gives $s_+ = 2$ so that (3.11) yields $\alpha = 3/2$. The asymptotic behavior of the solutions at infinity are

$$u_\lambda(x) \sim \eta x^{-1/2} \exp(-(x^2/2)), \qquad x \to \infty. \tag{3.21}$$

Since the coefficients are analytic in the right half-plane and both (3.15) and (3.16) are satisfied either of the maps $\phi_2$ or $\phi_3$ may be employed for this example. To see why the map $\phi_3$ is preferred, recall that the quantity $N_2(w)$ in (2.6) was required to be finite. The first term on the right-hand side of (2.6) for the present example takes the form

$$N = \int_\gamma^\infty |w(t+is)|^2\, dt = \int_B^\infty |w(t+is)|^2\, dt + I, \tag{3.22}$$

where the integral $I$ has no effect on the behavior of $w$ at positive infinity. If $B$ in (3.22) is sufficiently large so that (3.21) may be used in (3.22) then, upon recalling the change of variable (2.17),

$$N - I = \eta \int_B^\infty \left| e^{-(t+is)} \exp\left( \frac{-1}{2} e^{2(t+is)} \right) \right|^2 dt$$

$$= \eta \int_B^\infty e^{-t} \left| \exp\left( \frac{-1}{2} e^{2t}(\cos 2s + i \sin 2s) \right) \right|^2 dt$$

$$= \int_B^\infty e^{-t} \left| \exp\left( \frac{-1}{2} e^{2t} \cos 2s \right) \right|^2 dt.$$

TABLE VI

| True eigenvalues | 4 | 8 | 16 | 24 | $= M$ |
|---|---|---|---|---|---|
| $\lambda_p$ | 0.433–2 | 0.454–3 | 0.188–4 | 0.163–5 | = AEM |
| | | | $\lvert\mu_p - \lambda_p\rvert$ | | |
| 5 | 0.831–2 | 0.513–4 | 0.321–6 | 0.304–8 | |
| 9 | — | 0.168–2 | 0.607–6 | 0.194–7 | |
| 12 | — | — | 0.177–4 | 0.496–7 | |
| 16 | — | — | — | 0.331–5 | |

The latter is finite if $\cos 2s > 0$ or $0 < s < \pi/4$. Hence, for the map $\phi_2$ for this example select $d = \pi/4$. For the map $\phi_3$ one may select $d = \pi/2$ and, as in the previous example, the larger $d$ governs the choice of the map. It should be remarked that the accuracy exhibited in Table VI could be obtained using the $\phi_2$ map but the size of $M$ (and $N$) would be quite a bit larger. Indeed, if the results in Table VI are compared with the results in [7] (there the map $\phi_2$ was used) the superiority (with respect to economy of computation) of the map $\phi_3$ for this example is clearly seen.

EXAMPLE 3.7. (Rational) $-u''(x) + ([n(n+1))\, x^2 - n]/(x^2+1)^2)\, u(x) = \lambda u/(x^2+1)$, $u(0) = u(\infty) = 0$.

For each integer $n \geqslant 2$, this equation has a finite set of eigenvalues $\lambda_j = j \cdot (2n - j + 1)$ for $j = 2i - 1$ $(i = 1, 2, \ldots, [\![(n+1)/2]\!])$. Corresponding to each eigenvalue $\lambda_j$ the eigensolution is given by

$$u_{\lambda_j}(x) = \frac{P_j(x)}{(x^2+1)^{n/2}}, \tag{3.23}$$

where $P_j$ is a polynomial of exact degree $j$. An explicit representation of the $P_j$ as well as a number of their properties (including their relationship to the Tschebyscheff polynomials) is developed in [3].

TABLE VII

| True eigenvalues | 4 | 8 | 16 | 24 | $= M$ |
|---|---|---|---|---|---|
| $\lambda_p$ $(n=4)$ | 0.432–1 | 0.117–1 | 0.187–2 | 0.455–3 | = AER |
| | 0.239–0 | 0.109–0 | 0.183–1 | 0.325–2 | $= Q$ |
| | | | $\lvert\mu_p - \lambda_p\rvert$ | | |
| 8 | 0.139 + 1 | 0.562–0 | 0.615–1 | 0.849–2 | |
| 18 | 0.204 + 1 | 0.348–0 | 0.257–1 | 0.435–2 | |

An inspection of the inequality (3.15) combined with (3.23) shows that the former is satisfied with $\alpha = \frac{1}{2}$ ($P_1(x) = x$ for all $n$) and $\beta = n$. Hence the parameters (3.7) and (3.8) are $h = \pi/\sqrt{M}$ and $N = [\![M/2n]\!]$, respectively. Due to the nonexponential behavior of the solutions $u_{\lambda_j}$ in (3.23) there is no $\beta$ so that (3.16) is satisfied. Hence, the Table VII is obtained using the map $\phi_2(x)$. Note that the function $q(x)$ is negative on the initial segment $(0, (n+1)^{-1/2})$ of $(0, \infty)$. However, as in Example 3.3,

$$\liminf_{x>0} \left\{ \frac{q(x)}{(\phi_2'(x))^2} \right\} > \frac{1}{4}$$

so that the results of Theorem 2.1 are applicable to this example. Finally, following the comments preceding Example 3.1, the quantity $Q = M^{3/2} |\cos \theta_p| \exp(-(\pi d \alpha M)^{1/2})$ has been included in Table VII.

## ACKNOWLEDGMENTS

The authors thankfully acknowledge the careful reading and helpful suggestions made by the referees. A thank you also goes to Mrs. Susie Gray for her patient and skillful technical typing.

## REFERENCES

1. G. BLANCH, *Tables Relating to Mathieu Functions* (Columbia Univ. Press, New York, 1951), p. 24.
2. J. P. BOYD, *J. Comput. Phys.*, in press.
3. N. EGGERT AND J. LUND, *Appl. Anal.* **18**, 267 (1984).
4. S. FLUGGIE, *Practical Quantum Mechanics I* (Springer-Verlag, New York, 1971), p. 162.
5. D. GOTTLIEB, AND S. A. ORSZAG, *Numerical Analysis of Spectral Methods: Theory and Applications* (SIAM Philadelphia, PA, 1977).
6. J. LUND, *Math. Comput.* **47**, 1 (1986).
7. J. R. LUND AND B. V. RILEY, *IMA J. Numer. Anal.* **4**, 83 (1984).
8. F. W. J. OLIVER, *Asymptotics and Special Functions* (Academic Press, New York, 1974).
9. B. N. PARLETT, *The Symmetric Eigenvalue Problem* (Prentice-Hall, Englewood Cliffs, NJ, 1980), p. 304.
10. S. W. SCHOOMBIE AND J. F. BOTHA, *IMA J. Numer. Anal.* **1**, 47 (1981).
11. B. W. SHORE, *J. Chem. Phys.* **58**, 3855 (1973).
12. F. STENGER, Math. Comput. **33**, 85 (1979).
13. F. STENGER, *SIAM Rev.* **23**, 165 (1981).